Microwave Amplifier With Substrate Integrated Waveguide Bandpass Filter Matching Network

Phanam Pech, *Graduate Student Member, IEEE*, Phirun Kim, *Member, IEEE*, and Yongchae Jeong, *Senior Member, IEEE*

***Abstract*— This letter presents a microwave amplifier (MA) with a substrate integrated waveguide (SIW) bandpass filter (BPF) output matching network (OMN). The codesigned amplifier and SIW BPF with complex termination impedance (CTI) can reduce the circuit size and the design complexity while improving loss. To match the CTI of the SIW BPF, the frequencies of the first and/or last resonators must be detuned. Moreover, the proposed SIW BPF OMN can be designed for Chebyshev characteristics in either odd- or even-ordered resonators. For validation, the MA with the proposed SIW BPF OMN was designed at 10 GHz. High-frequency selectivity is obtained by using the proposed SIW BPF OMN along with conventional MA performances.**

***Index Terms*— Bandpass filter (BPF), power amplifier, substrate integrated waveguide (SIW).**

I. Introduction

THE coupled resonators substrate integrated waveguide (SIW) bandpass filter (BPF) with real and/or complex termination impedances (CTIs) is an important circuit used in most microwave applications for the purpose of directly matching the adjacent circuits with relatively high-power handling. The arbitrary CTI matching networks with a BPF response using $\lambda/4$ stepped impedance resonators have been proposed in [1]. A new synthesis method of SIW BPF for even-order Chebyshev response was analyzed to avoid impedance mismatching and proposed in [2]. In addition, an arbitrary real-to-real impedance transformer SIW BPF using a coupled resonator was proposed in [3]. Recently, the CTI BPF has been proposed, and its potential applications have been outlined. The codesigned cavity resonators of the CTI BPF and microwave amplifiers (MAs) have been designed at the center frequencies (f_0) of 1.22 [4], 3 [5], and 3.1 GHz [6]. These BPFs were, respectively, designed for one-, two-, and three-resonators using a coupling matrix and transformed into the physical design with substrate-integrated evanescent-mode (EVA) cavities.

In this letter, the design of MA with SIW BPF output matching network (OMN) is proposed. The proposed BPF OMN can be designed easily by using J-inverter with either odd or even order and arbitrary input and output impedances (Z_{in}, Z_{out}). Using the codesigned MA with the proposed SIW BPF OMN provides better electrical performances, a reduced circuit size, and a simpler design than using the conventional MA (CMA) cascaded with the transmitting SIW BPF.

Manuscript received December 1, 2020; revised January 26, 2021; accepted February 11, 2021. Date of publication February 16, 2021; date of current version April 8, 2021. This research was supported by Research Base Construction Fund Support Program, funded by Jeonbuk National University in 2020. *(Corresponding author: Yongchae Jeong.)*

Phanam Pech and Yongchae Jeong are with the Division of Electronics and Information Engineering, IT Convergence Research Center, Jeonbuk National University, Jeonju-si 54896, South Korea (e-mail: ycjeong@jbnu.ac.kr).

Phirun Kim is with the Assistant of the Ministry of Post and Telecommunications, Ministry of Post and Telecommunications, Phnom Penh 12202, Cambodia.

Color versions of one or more figures in this letter are available at https://doi.org/10.1109/LMWC.2021.3059859.

Digital Object Identifier 10.1109/LMWC.2021.3059859

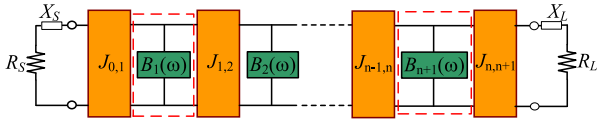

Fig. 1. Generalized CTI BPF with admittance inverters.

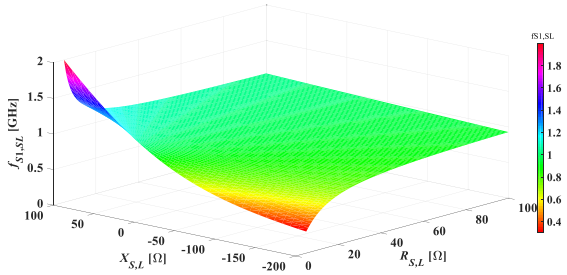

Fig. 2. Detuned frequency trajectory according to real and imaginary values of CTI.

II. Design Equation

Fig. 1 shows the generalized CTI BPF with admittance inverters, where the CTIs are $Z_S = R_S \pm jX_S$ and $Z_L = R_L \pm jX_L$, respectively. This BPF can be designed for either real-to-real, real-to-complex, or complex-to-complex impedances with n-stage coupled resonators. The complex impedance cannot be directly matched to the adjacent J-inverters. To address this, the first and last resonators must be detuned to the resonance frequencies to match the reactive parts of the termination impedances. Depending on the complex reactance, the detuned frequency can be defined as follows [7]:

$$f_{S1,Ln} = f_0 \left[\sqrt{1 + \left(\frac{X_{S,L}\text{FBW}}{2R_{S,L}g_{0,n}g_{1,n+1}} \right)^2} + \frac{X_{S,L}\text{FBW}}{2R_{S,L}g_{0,n}g_{1,n+1}} \right] \tag{1}$$

where f_{S1} and f_{Ln} are the new resonance frequencies of the first and last resonators, respectively. Fig. 2 shows the detuned frequency trajectory according to the real and imaginary values of the CTIs. When the imaginary parts of the source and load impedances are both zeros, $f_{S1} = f_{Ln} = f_0$ is obtained. Similarly, the frequency is detuned to lower and higher frequencies for $X_{S,L} < 0$ and $X_{S,L} > 0$, respectively. After determining the detuned frequencies of the first and the

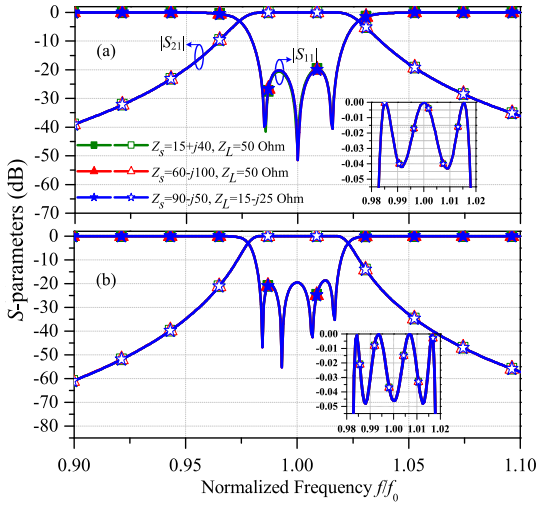

Fig. 3. S-parameter and equal-ripple characteristics according to arbitrary CTIs: (a) three-stage and (b) four-stage.

last resonators, the J-inverters of the coupled-resonator can be defined as follows:

$$J_{01} = \sqrt{\frac{\text{FBW}b_1}{R_S g_0 g_1}}, \quad J_{i,i+1} = \text{FBW}\sqrt{\frac{b_i b_{i+1}}{g_i g_{i+1}}},$$
$$J_{n,n+1} = \sqrt{\frac{\text{FBW}b_n}{R_L g_n g_{n+1}}} \quad i = 1, 2, 3, \ldots, n-1. \quad (2)$$

By arbitrarily choosing inductor L_i, the capacitance of the parallel resonator can be found with $C_i = 1/\omega^2 L_i$. Next, the slope parameters of the first, intermediate, and last resonators can be found with $b_1 = 2\pi f_{S1} C_1$, $b_i = \omega_0 C_i$, and $b_n = 2\pi f_{Ln} C_n$. The coupling coefficient ($K_{i,i+1}$) of the resonator and the external quality factors ($Q_{S1,Ln}$) of the first and last coupled-resonators are defined as follows [8]:

$$K_{i,i+1} = \frac{J_{i,i+1}}{\sqrt{b_i b_{i+1}}}, \quad Q_{S1} = \frac{b_1}{R_S J_{01}^2}, \quad Q_{Ln} = \frac{b_n}{R_L J_{n,n+1}^2}. \quad (3)$$

For the analysis, the BPFs are designed for the Chebyshev response with a passband ripple of 0.0436 dB ($|S_{11}| = -20$ dB) and fractional bandwidth (FBW) = 3.5%. The S-parameters and the equal-ripple characteristics of the proposed BPFs with $n = 3$ and $n = 4$ for different CTIs are, respectively, shown in Fig. 3(a) and (b). The results of the simulations indicate that the proposed BPF can be designed with odd- or even-order resonators and CTI.

The SIW BPF with CTI is designed by using the magnetic coupling with via-hole windows [2]. The Q_{S1} and Q_{Ln} can be extracted or calculated from the electromagnetic (EM) simulation using the following equation:

$$Q_{S\_\text{EM},L\_\text{EM}} = \frac{f_{S1,Ln}}{\Delta f_{\pm 3\text{ dB}}} \quad (4)$$

where $\Delta f_{\pm 3\text{ dB}}$ is a 3-dB bandwidth. Similarly, the coupling coefficient between the intermediate resonators can be extracted from the EM simulation by using (5) for synchronously tuned coupling resonators

$$K_{i,i+1} = \pm\frac{f_{p_2}^2 - f_{p_1}^2}{f_{p_2}^2 + f_{p_1}^2} \quad (5)$$

where f_{p1} and f_{p2} are the two split resonant frequencies, respectively.

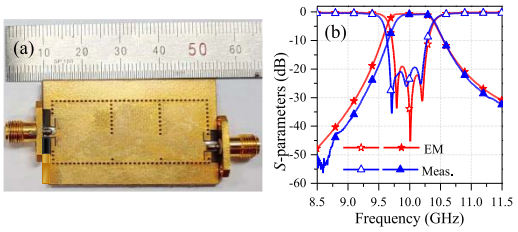

Fig. 4. 50-to-50-Ω SIW BPF: (a) circuit and (b) frequency response.

III. SIW BPF and MA Designs

A. CMA Design

For experimental validation, three different MAs were designed with different OMNs by using the GaN HEMT transistor, CGHV1F006S from Wolfspeed. Under the bias conditions of $V_{GS} = -2.85$ V, $I_{DQ} = 4$ mA, and $V_{DS} = 35$ V, the optimum input (Z_{Source}) and output (Z_{Load}) impedances at $f_0 = 10$ GHz are $11.48 + j79.86\ \Omega$ and $6.87 + j0.6\ \Omega$, respectively. The CMA was designed with a conventional matching network (CMN). The CMN was realized by using the balanced open-stubs with series transmission line (TL).

The 50-to-50-Ω SIW BPF could be designed by using the derived equations. In this design, FBW = 3.5% with a passband ripple of 0.0436 dB and a three-pole filter were chosen. The equality of $f_{S1} = f_{Ln} = f_0$ could be obtained from (1). From (2), $J_{01} = J_{34} = 0.00511$ and $J_{12} = J_{23} = 0.001148$ were calculated. The physical dimensions of the SIW BPF can be obtained by following a similar approach in [2] and [3].

B. MA Design With Proposed CTI SIW BPF OMN

Since the SIW BPF is grounded with the via-holes, the bias-circuit with a dc-block is essentially realized as small as possible. The SIW BPF OMN was designed with CTIs of Z_{out} and 50 Ω. From electrical simulation with Advanced Design System (ADS) software, $Z_{\text{out}} = 41.415 - j125.2\ \Omega$ was obtained. From (1), f_{S1} was calculated and detuned to 10.639 GHz. After choosing $L_1 = L_2 = L_3 = 0.5$ nH, $C_1 = 0.4476$ pF and $C_2 = C_3 = 0.5066$ pF were calculated. Then, $J_{01} = 0.005443$, $J_{12} = 0.001113$, $J_{23} = 0.001148$, and $J_{34} = 0.00511$ were calculated from (2). The coupling windows of the resonators were located on the bottom to improve frequency selectivity [9]. On the other hand, the bandwidth of MA can be extended by increasing the FBW of SIW BPF OMN.

IV. Simulation and Measurement Results

The SIW BPFs were designed and implemented on RT/Duriod 5880 substrate with $\varepsilon_r = 2.2$ and $h = 0.787$ mm. Similarly, the MAs were designed on an RT/Duriod 5880 substrate with $h = 0.254$ mm.

The photograph and the frequency response of the 50-to-50-Ω termination SIW BPF are, respectively, shown in Fig. 4(a) and (b). At f_0, the measured insertion loss is 0.83 dB. Similarly, the layout and the dimensions of the proposed OMN are shown in Fig. 5(a). The matching impedances observed from the transistor connection point and the S-parameter responses of the proposed OMN are shown in Fig. 5(b) and (c), respectively. The optimum load impedance matching was obtained at f_0 with the measured insertion loss of 1.25 dB.

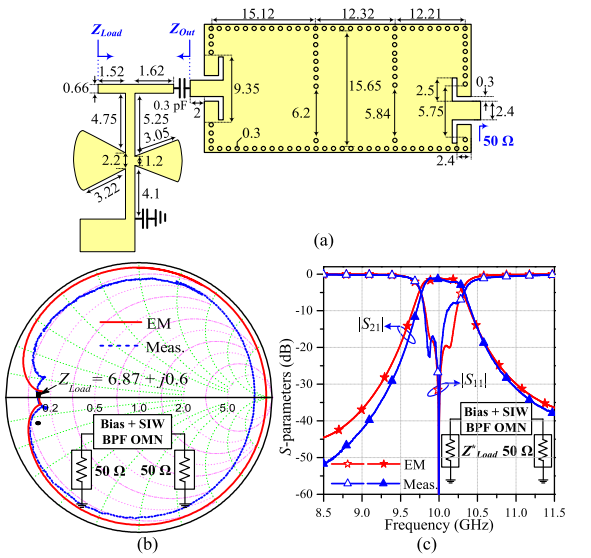

Fig. 5. Proposed SIW BPF with bias line: (a) layout/dimensions, (b) matching impedance point, and (c) S-parameter responses.

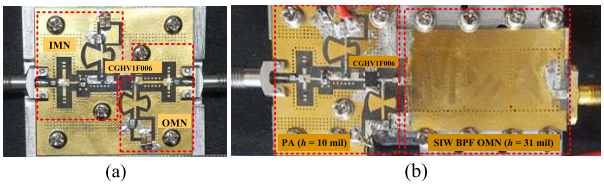

Fig. 6. Fabricated MAs: (a) CMA and (b) MA with SIW BPF OMN.

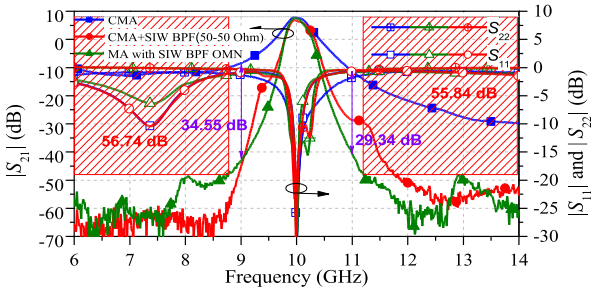

Fig. 7. S-parameters comparison of fabricated MAs.

Photographs of the fabricated MAs are shown in Fig. 6. During the experiment, the CMA was cascaded with a 50-to-50-Ω SIW BPF through an SubMiniature version A (SMA) adaptor, where the insertion of an SMA adaptor was deembedded for the evaluation of the electrical performances. Fig. 7 shows the measured S-parameters of three MAs within the frequency range from 6 to 14 GHz. The small-signal gains of CMA, CMA with 50-to-50-Ω SIW BPF, and MA with the proposed SIW BPF OMN are 7.73, 6.93, and 7.42 dB, respectively, at f_0. However, by using the proposed SIW BPF OMN, maximum attenuations over 55.84 dB from the passband can be obtained.

For the output power test, the continuous-wave (CW) signal was used in the measurement. The results over the frequency range from 9.8 to 10.2 GHz are shown and compared in Fig. 8. At f_0, the measured output power (P_{out}) and the saturation gain (G_{sat}) of the CMA are 35.86 dBm and 6.13 dB, respectively. Similarly, P_{out} and G_{sat} of the CMA cascaded with the 50-to-50-Ω SIW BPF are decreased to 34.13 dBm and 5.02 dB, respectively, due to the additional loss of the SIW BPF and not perfect matching between CMA and 50-to-50-Ω SIW BPF. However, P_{out} and G_{sat} of the proposed MA with

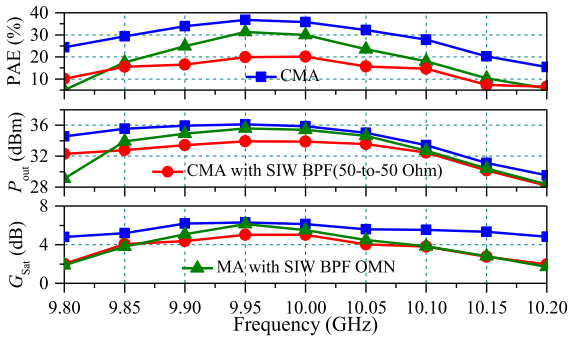

Fig. 8. PAE, output power, and saturation gain of measured amplifiers over a 400-MHz bandwidth.

TABLE I

COMPARISON OF MEASUREMENT RESULTS AT CENTER FREQUENCY

	P_{out} (dBm)	G (dB)	PAE (%)	Size (mm^2)
CMA	35.86	6.13	35.74	41.89 × 44.52
CMA+SIW BPF (50-50 Ω)	34.13	5.02	23.74	41.89 × 108.24
MA+SIW BPF OMN	35.42	5.49	29.38	41.89 × 78.54

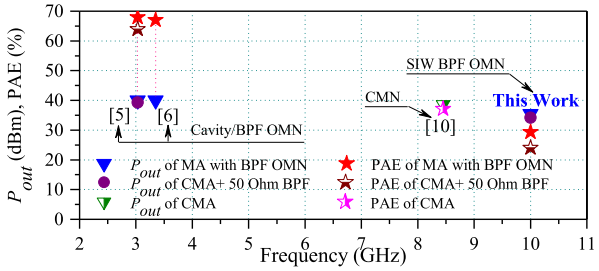

Fig. 9. P_{out} and PAE comparisons with state-of-the-art MAs.

the SIW BPF OMN are 35.42 dBm and 5.49 dB, respectively. At f_0, the PAEs of the CMA, the CMA cascaded with the 50-to-50-Ω SIW BPF, and the MA with the SIW BPF OMN are 35.74%, 23.74%, and 29.38%, respectively.

The measured performances are summarized in Table I. The MA with the SIW BPF OMN provides better performances than the CMA cascaded with the 50-to-50-Ω SIW BPF; moreover, its circuit size is reduced by about 28%.

The performances of the proposed MA are compared with those of the state-of-the-art amplifiers in Fig. 9. The proposed MA is designed on a simple microstrip line at the *X*-band using the CTI SIW BPF, which is a cheap design process. Because the frequency selectivity was not considered in [10], the output power and the efficiency would be degraded when connected with BPF. Furthermore, since [5] and [6] were realized with a cavity-type BPF OMN, the fabrication process would be more difficult. In [5], the PAE of the codesigned MA with BPF OMN is improved by around 4% over the PAE of CMA cascaded with a 50-to-50-Ω BPF. Similarly, the PAE of the proposed MA with SIW BPF OMN is improved by about 5.6% over that of CMA cascaded with a 50-to-50-Ω SIW BPF.

V. CONCLUSION

A new design approach of a MA with a CTI SIW BPF OMN is proposed and investigated in this letter. The proposed MA can remove a transmitting BPF cascaded from the amplifier or relax the specifications of the transmitting BPF. The insertion loss, the overall circuit size, and the complexity of the transmitter in the RF front end can also be improved. Altogether, the electrical results indicate that the proposed CTI BPF design method can be applied to microwave circuit and system designs.

REFERENCES

[1] P. Kim and Y. Jeong, "A new synthesis and design approach of a complex termination impedance bandpass filter," *IEEE Trans. Microw. Theory Techn.*, vol. 67, no. 6, pp. 2346–2354, Jun. 2019.

[2] K. Wang, S.-W. Wong, G.-H. Sun, Z. N. Chen, L. Zhu, and Q.-X. Chu, "Synthesis method for substrate-integrated waveguide bandpass filter with even-order Chebyshev response," *IEEE Trans. Compon., Packag., Manuf. Technol.*, vol. 6, no. 1, pp. 126–135, Jan. 2016.

[3] J. Jeong, P. Kim, P. Pech, Y. Jeong, and S. Lee, "Substrate-integrated waveguide impedance matching network with bandpass filtering," in *Proc. IEEE Radio Wireless Symp. (RWS)*, Jan. 2019, pp. 1–3.

[4] K. Chen, X. Liu, W. J. Chappell, and D. Peroulis, "Co-design of power amplifier and narrowband filter using high-Q evanescent-mode cavity resonator as the output matching network," in *IEEE MTT-S Int. Microw. Symp. Dig.*, Jun. 2011, pp. 1–4.

[5] K. Chen, J. Lee, W. J. Chappell, and D. Peroulis, "Co-design of highly efficient power amplifier and high-Q output bandpass filter," *IEEE Trans. Microw. Theory Techn.*, vol. 61, no. 11, pp. 3940–3950, Nov. 2013.

[6] K. Chen, T. Lee, and D. Peroulis, "Co-design of multi-band high-efficiency power amplifier and three-pole high-Q tunable filter," *IEEE Microw. Wireless. Compon. Lett.*, vol. 23, no. 12, pp. 647–649, Dec. 2013.

[7] D. Swanson and G. Macchiarella, "Microwave filter design by synthesis and optimization," *IEEE Microw. Mag.*, vol. 8, no. 2, pp. 55–69, Apr. 2007.

[8] G. L. Matthaei, L. Yong, and E. M. T. Jones, *Microwave Filter, Impedance-Matching Networks, and Coupling Structures*. New York, NY, USA: McGraw-Hill, 1964.

[9] Y. D. Dong, W. Hong, and H. J. Tang, "A novel millimeter wave substrate integrated waveguide filter using TE301 mode cavities," in *Proc. Global Symp. Millim. Wave*, 2008, pp. 91–93.

[10] W. S. Waldstein, A. M. B. Kortright, and N. R. Simons, "Multiband reconfigurable harmonically tuned GaN SSPA for cognitive radios," in *Proc. NASA/TM*, 2017, pp. 1–7.